*36th EPS Conference on Plasma Phys. Sofia, June 29 - July 3, 2009 ECA Vol.**33E**, P-5.144 (2009)*

Studies of mechanisms of transport barrier formation in RF discharge plasmas of the Uragan-3M torsatron

V. I. Tereshin, A. A. Beletskii, P. Ya. Burchenko, V. V. Chechkin, L. I. Grigor'eva, A. Ye. Kulaga, A. V. Lozin, Yu. K. Mironov, V. L. Ocheretenko, V. K. Pashnev, V. S. Romanov, A. I. Skibenko, A. S. Slavnyj, Ye. L. Sorokovoy, Ye. D. Volkov

Institute of Plasma Physics, National Science Center "Kharkov Institute of Physics and Technology", 61108 Kharkov, Ukraine

Introduction. A reduction of the anomalous transport and bringing transport coefficients to the collisional level in magnetic confinement systems are necessary for creation of the fusion reactor. This can be realized by formation of the internal (ITB) and/or edge (ETB) transport barriers where the turbulence is suppressed by the radial E_r shear and the corresponding sheared poloidal plasma flow [1]. The origin of ITB in stellarators is facilitated by low order rational surfaces (RS) [2]. The most interesting mechanism of ITB formation is initiated by the collisionless non-ambipolar electron loss near RS and generation of a strong $E_r > 0$ (neoclassical electron root). To realize this, a hot electron plasma is necessary. Formation of ITB (H-mode confinement) is associated with occurring a layer with a strong $E_r < 0$ at the plasma boundary and the corresponding radial current. In particular, such a current can be driven by a non-ambipolar ion loss [3, 4] or be generated by a biased electrode [5].

In this report, possible mechanisms of ITB and ETB formation in the Uragan-3M (U-3M) torsatron are elucidated.

Effects arising with transition to the improved confinement regime in U-3M. The magnetic configuration of the U-3M torsatron (l = 3, m = 9, R = 1 m, $\bar{a} \approx 0.12$ m, $\iota(\bar{a})/2\pi \approx 0.3$, B_ϕ = 0,7 T) with an open helical divertor is characterized by three main chains of magnetic islands $\iota/2\pi = 1/4$ [6,7] (Fig. 1). A hydrogen plasma is RF produced and heated at the frequency 8.8 MHz ($\omega = 0{,}8\omega_{ci}(0)$) in the multi-mode Alfven resonance regime [8]. A two-temperature ion distribution with a suprathermal ion (STI) tail sets in during the heating. Under typical conditions, the RF power fed to the antenna is P~200 kW, $\bar{n}_e \sim (1\div2)\times10^{12}$ cm^{-3}, T_{i1}~50÷80 eV, T_{i2}~300 eV, and the STI tail extends to ~2000 eV. The electron temperature in the center can attain ~600 eV and fall to ~50 eV at the boundary.

If the power P, a fraction of it being spent for plasma heating, is high enough ($\gtrsim$170 kW at $\bar{n}_e \approx 1.2\times10^{12}$ cm^{-3}), spontaneous changes in RF discharge plasma parameters are observed in the middle part of the RF pulse (t = 28 ms in Fig. 2), such as a rise of the energy content (Fig. 2a), density (Fig. 2b), electron cyclotron emission (Fig. 2c), etc. These changes resulting from the T_e rise, indicate a transition to the improved confinement mode (hereinafter, "transition") and are characteristics of all tokamaks and stellarators with transition [1]. In U-3M the transition is preceded by an increase of fast ion content (FI: T_{i2} group + STI) (Fig. 2d) and by a short-time enhanced plasma outflow (Fig. 2e) and an accompanying ejection of FI to the divertor (Fig. 2f, energies >500 eV) on the ion ∇B side.

According to estimations based on the increment of the energy content, the time τ_E can increase 1.5÷2 times with the transition (up to ~5 ms).

Indications of ITB are [9] a reduction of the level of small-scale density fluctuations in the core plasma (Fig. 3), a broadening of the $\bar{n}_e(r)$ profile and its flattening in the center (Fig. 4) and a sharpening of the $T_e(r)$ profile (Fig. 5). These changes are accompanied by formation of pedestals in the $\bar{n}_e(r)$ and $T_e(r)$ profiles, their positions being consistent with the island

structure. The radial E_r gradients are subjected to a strong steepening between the islands (Fig. 6). All this confirms a determining role of RS in ITB formation.

The E_r profile at the plasma boundary which is a characteristic of ETB arises as a result of a hard E_r bifurcation toward a more negative value and formation of a layer with a strong E_r shear [10] and, accordingly, the shear of poloidal rotation velocity $\boldsymbol{E}\times\boldsymbol{B}$ where the density (Fig. 7b) and electric field (Fig. 7c) fluctuations and the fluctuation-induced radial particle flux (Fig. 7d) giving rise to the anomalous transport are partly or completely damped.

It follows from Fig. 2d,f that the FI content passing over a maximum and the burst of FI outflow to the divertor occur not only in the middle of the RF pulse but at the start of discharge, in the phase of density rise (phase 1), too. Corresponding density values, $\overline{n}_{e1}$ and $\overline{n}_{e2}$, are close at both stages of the discharge, $\overline{n}_{e1} \approx \overline{n}_{e2} \approx 1.2\times10^{12}$ cm^{-3}. This suggests an idea that an H-like mode exists at the phase 1 too. Such an idea is validated by the character of time evolution of the edge floating potential, V_f, in phase 1 and in the middle of the discharge (phase 2) (Fig. 8) and by comparison of the V_f profiles in different phases (Fig. 9). As follows from Fig. 8, after discharge ignition potential fluctuation occurs synchronously with the FI burst (t = 6 ms) and the density increases from $\overline{n}_{e1}$ to $\overline{n}_{e3} \cong 2.4\times10^{12}$ cm^{-3} at t = 8 ms. Here, a hard (first) potential bifurcation toward a higher value occurs and the fluctuation level increases, thus indicating termination of the supposed H-mode state in phase 1. Nearly at the same time, a density decay starts (phase 2). The phase 2 is terminated by a (second) potential bifurcation toward a lower value at $\overline{n}_{e2} \cong 1.2\times10^{12}$ cm^{-3} $\approx \overline{n}_{e1}$ and H-mode resumption (phase 3). The variations of the edge potential with transition from phase 1 to phase 2 (Fig. 9a) and with reverse transition from phase 3 to phase 2 (Fig. 9b) are qualitatively similar. The edge gradient $\delta E_r/\delta r$ at the start of phase 3, as estimated by Fig. 9b data, is obviously stronger than that before the end of phase 2 (-1820 and -490 V/cm^2, respectively) and, consequently, should make a more stronger damping effect on the fluctuations. A qualitatively similar relationship between the gradients takes place at the phase 1 to phase 2 transition (Fig. 9a), though the absolute $\delta E_r/\delta r$ values are less in this case (-520 and -219 V/cm^2, respectively).

The density rise in phase 1 results in the termination of the state with stronger E_r shear. The reduction of $\delta E_r/\delta r$ should in turn result in a turbulence increase and the turbulence-induced anomalous transport. This, probably, explains the density decay in phase 2. In the Fig. 8 conditions, the density $\overline{n}_{e3}$ is ~2 times higher than $\overline{n}_{e1}$, i.e., a hysteresis of the reverse transition is observed.

The value of $\overline{n}_{e3}$ depends on P. The $\overline{n}_{e3}(P)$ plot is shown in Fig. 10 together with the P-dependences of $\overline{n}_{e1}$ (in fact, no dependence on P) and the FI burst amplitude I_i in phase 1. The H-mode exists in the interval between $\overline{n}_{e1}$ and $\overline{n}_{e3}$. It follows from Fig. 10 that (1) a threshold heating power exists corresponding to $P \approx 170$ kW and (2) the enhanced short-time FI outflow to the divertor exists at the power less than the threshold one too, i.e., it is a primary effect in the supposed casualty between the FI loss and H-transition.

Summary. Characteristic changes in the n_e and T_e profiles with formation of pedestals with transition to the improved confinement regime confirm the ITB formation. The relation of ITB to the RS follows from the apparent tieing of the pedestal radial position to the magnetic islands and the strong E_r shear in the interisland space.

The data obtained indicate that the H-mode transition is initiated by the FI loss. As a first original model predicting the E_r bifurcation under the effect of FI ion loss with heating power increase (in a tokamak), the balance of the ion orbit loss with the non-ambipolar electron flow caused by the edge turbulence is considered (see the review paper [11]). In another original model [3] which seems more adequate to the U-3M conditions, E_r is found from the condition

where the changes of the poloidal momentum due to the FI orbit loss (the T_{i2}+STI ions, in our case) are balanced with the neoclassical damping for the account of the poloidal viscosity due to slower ions in the plateau regime (group T_{i1}). As a continuation of ideas developed in [3], it is shown theoretically in [4] that in non-asymmetric systems (stellarators) the poloidal velocity $\boldsymbol{E}\times\boldsymbol{B}$ can also be carried to bifurcation by the radial drift-orbit flux driven by collisionless helically trapped ions.

References

[1] F. Wagner *et al.* Plasma Phys. Control. Fusion 48 (2006) A217.
[2] C. Hidalgo *et al*., J. Plasma Fusion Res. SERIES **4** (2001) 167.
[3] K. C. Shaing, E. C. Crume, Jr., Phys. Rev. Lett. **63** (1989) 2369.
[4] Shaing K. C., Phys. Rev. Lett. **76** (1996) 4364.
[5] R. R. Weynants, R. J. Taylor, Nucl. Fusion 30 (1990) 945.
[6] G. G. Lesnyakov *et al*., Nucl. Fusion **32** (1992) 2157.
[7] V. N. Kalyuzhnyj, V. V. Nemov, Fusion Sci. Technol. 46 (2004) 248.
[8] O. M. Shvets *et al*., Nucl. Fusion **32** (1986) 23.
[9] Ye. D. Volkov *et al*. Czech. J. Phys. **53** (2003) 887.
[10] V. V. Chechkin *et al*. Plasma Phys. Control. Fusion **48** (2006) A241.
[11] J. W. Connor, H. R. Wilson, Plasma Phys. Control. Fusion 42 (2000) R1.

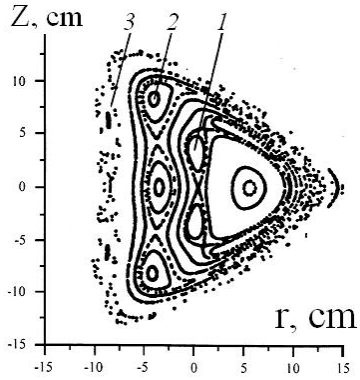

Fig. 1. Field line structure in a symmetric poloidal cross-section. *1, 2, 3* – magnetic islands ι/2π=1/4.

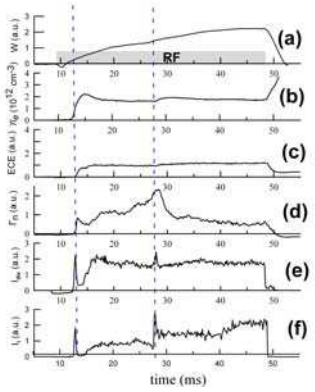

Fig. 2. (a) energy content; (b) density $\overline{n}_e$; (c) 2-nd harmonic ECE; (d) CX neutral flux (perpendicular energy 1350 eV); (e) plasma and (f) fast ion (>500 eV) outflows to the divertor on the ion ∇B drift side.

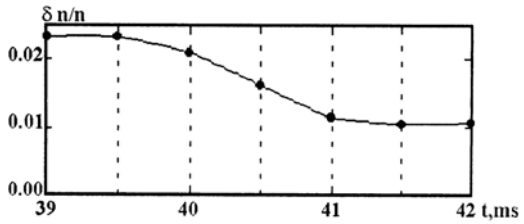

Fig. 3. Relative electron density fluctuation level in the core plasma. Transition occurs at 39.5 ms (measurements with a low time resolution).

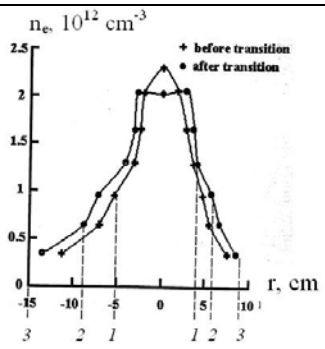

Fig. 4. Electron density profiles before and after the transition. *1, 2, 3* – magnetic island positions (see Fig. 1).

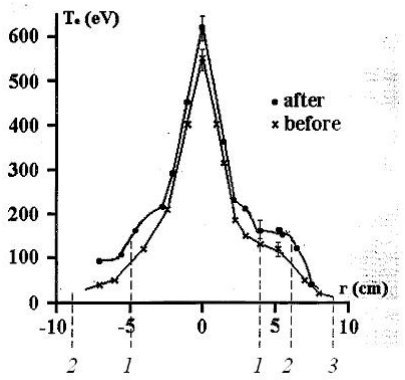

Fig. 5. Electron temperature profiles before and after the transition. *1, 2, 3* – magnetic island positions (see Fig. 1).

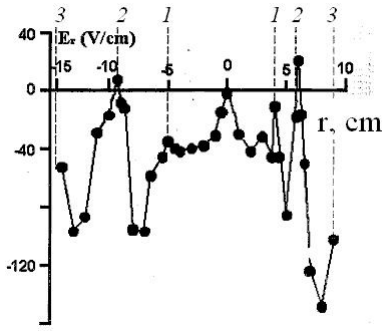

Fig. 6. Radial electric field radial distribution after the transition. *1, 2, 3* – magnetic island positions (see Fig. 1).

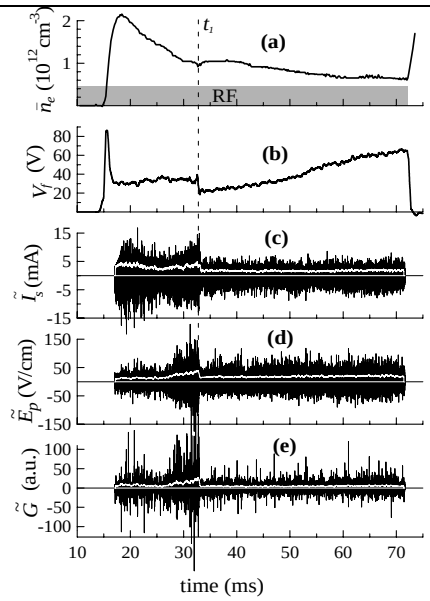

Fig. 7. (a) density $\bar{n}_e$; (b) edge floating potential; edge fluctuations of (c) density (ion saturation current); (d) poloidal electric field; (e) fluctuation-induced radial particle flux. Averaged levels are drawn in white in (c, d, e).

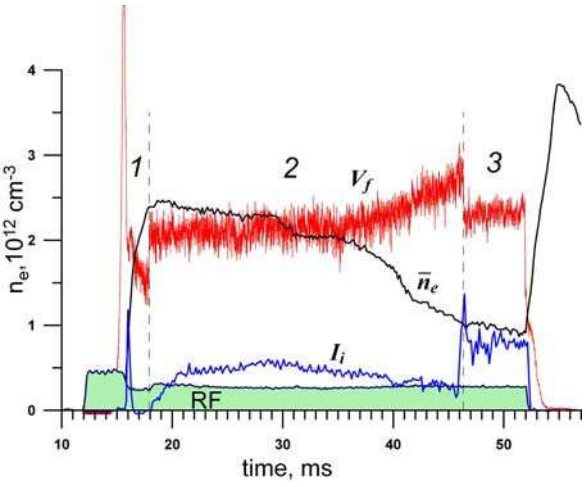

Fig. 8. Density $\bar{n}_e$, edge floating potential, V_f, and fast ion (>500 eV) outflow to the divertor on the ion ∇B drift side, I_i. *1, 2, 3* – phases of the discharge.

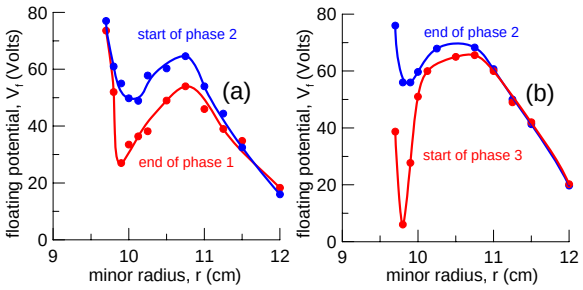

Fig. 9. Edge floating potential profiles before and after (a) 1st bifurcation, (b) 2nd bifurcation.

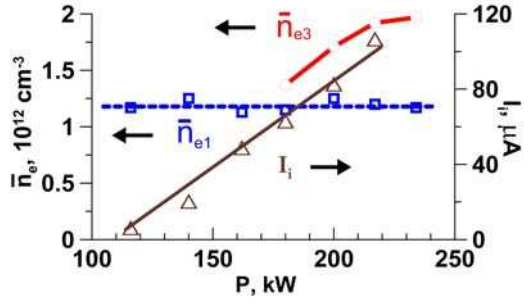

Fig. 10. Densities $\bar{n}_{e1}$, $\bar{n}_{e3}$ and amplitude of enhanced short-time fast ion outflow to the divertor, I_i, as functions of RF power fed to the antenna, P.